Fabrication of Polycaprolactone and Polylactic Acid Shapeless Scaffolds via Fused Deposition Modelling Technology

Amirsalar Khandan*, Saeid Esmaeili

Young Researchers and Elite Club, Khomeinishahr Branch, Islamic Azad University, Isfahan, Iran

ARTICLE INFO

Article history:

Received 26 November 2019
Accepted 8 April 2020
Available online 15 April 2020

Keywords:

Bone scaffold
Polycaprolactone
3D Printing
Polylactic Acid
Additive Manufacturing

ABSTRACT

The porous scaffold provides a temporary environment for bone growth and facilitates cell adhesion, cell growth and differentiation. In the present study, polymeric scaffolds were designed and fabricated via fused deposition modelling (FDM) method for orthopedic defect approaches using polycaprolactone (PCL) and polylactic acid (PLA) polymer. The prepared scaffold was coated with Chitosan-Hydroxyapatite (HA) as a reinforcement. The application of PLA, PCL and HA received attention of orthopedic surgeons to accelerate the bone healing. However, the comparison between the compression strength value of these scaffolds required more investigation and advance mechanical testing. In this study, we coat the novel PCL and PLA scaffold with chitosan-HA composite to mimic with humans' body. In the next stage, the mechanical strength and the biological response of the specimen were examined. Then, the morphology and phase characterization of the materials were analyzed using scanning electron microscopy (SEM) and X-ray diffraction (XRD) technique. The apatite formation and weight change test were performed on the porous scaffold which showed proper hydrophilicity. The microstructure of the porous scaffold was simulated using the Abaqus simulation with the extracted data from the experimental work. At the end, it was concluded that the most suitable scaffold was fabricated made of PLA filament and coated with chitosan-hydroxyapatite nanocomposite which can be useful choice for bone tissue engineering.

1-Introduction

Engineered hard porous tissues can reduce the need for tissue replacement and generally eliminate the need for organ transplants [1-2]. The bone injury with minimal treatment can be recover, but some damages, such as the complete disappearance of the bone caused by the tumor, union bone and infection of the lesions largely cannot be treated easily. These bone injuries often destroy much of the bone tissue and the natural mechanisms of the ossein. Restorative medicine is a branch of medical science that deals with such bone and hard tissue injuries [2-5]. One of the things that is constantly researched in bone tissue engineering is to explore different ways to expedite treatment as well as reduce side effects and minimize the disruptions caused by treatment methods in the patient's daily life [4-6]. This issue is also of great interest in topics such as bone fracture healing because the therapeutic process is highly disruptive to one's life and causes costly secondary surgeries in the patient [5-8]. One of the tools in regenerative medicine is

* Corresponding author:
E-mail address: sas.khandan@iaukhsh.ac.ir

transplantation of bone-like structures made by tissue engineering tools [7-8]. The goal of tissue engineering is to restore function of the bone by transmitting the living factors that integrate with the patient with new physiological tissue materials. The potential impact of tissue engineering field is much wider in medical domain [8-12]. For example, autografts are associated with problems such as donor deficiency and virus transmission, while allografts and xenografts are at risk of transmitting disease and immune response and synthetic substances that do not behave like normal bone [9-14]. It is important to note that the materials used in the fabrication of the scaffold needs to have suitable bioactivity property response with the host and guest tissue. The importance of natural polymers like chitosan, chitin, gelatin and sodium alginate in the preparation of porous bone scaffold is their clinical property due to their biocompatibility with other materials such as; digestibility, non-toxicity, high absorbency, and availability as a drug carrier [13-18]. Seitz et al. [19] conducted a three-dimensional (3D) print on a porous ceramic scaffold for bone substitute application with fully interconnected channels to repair bone defects. Fast prototyping, especially 3D printing, is well suited for the production of porous matrices directly from powdered materials. They used a modified HA to make 3D printing scaffold as a biocompatible implant for bone regeneration. The prototypes were successfully produced and identified using special materials characterization. It was shown that the essential parts can be made with internal channels and proper dimensions near 400-500 microns and wall structures up to 300-350 microns thickness. The mechanical strength of the designed part was about 22 MPa [19-25]. In recent years, research on new bone substitutes has focused on nonmetallic composite materials, especially polymer/ceramic, ceramic/ceramic and nanocomposite [26-28]. These composites consist of a polymeric and bioactive powder that provide suitable biological and mechanical properties for bone substitute applications. These materials relate the advantages of polymers such as structural stability, strength, biocompatibility, and optimum shape to ceramics that resemble to the human bone microstructure. The lack of adhesion between the HA particles and the polymer usually results in early failure in the two-phase joint elements [28-34]. In this project, we fabricated a novel chitosan-HA coated on PLA and PCL scaffold using FDM technology as a biocompatible material. Research has found the effectiveness of the above-mentioned method with high rate of success. The use of different scaffolds with biocompatible and biodegradable ingredients that can accelerate bone healing and damage the body.

2. Materials and Methods

The materials used to make the scaffolds and its coating along with the manufacturer as well as the chemical formula are listed in Table 1.

Table 1: Based materials for preparation of coating on porous PLA and PCL

Company	Chemical formula	Element
Aldrich, United States	$C_9H_{11}NO_4$	Chitosan
Merck, United States	$Ca_5(PO_4)_3(OH)$	Hydroxyapatite
TAT, Iran	CH_3COOH	Acetic acid

The description of the material properties, fabrication procedure and method of synthesis is also discussed in the following sections. Chitosan is one of the most important natural biopolymers with the linear polysaccharide structure which synthesized from chitin with random units of d-glucosamine and n-acetyl d-glucosamine. The PLA and PCL scaffolds coated with chitosan-HA. In order to synthesize the chitosan-hydroxyapatite hydrogel, chitosan was first incubated in 100 mL distilled water containing (1 vol%) of acetic acid at 50°C on a magnetic stirrer for several hours to completely dissolved for 60 min on IKA stirrer according to Figure 1.

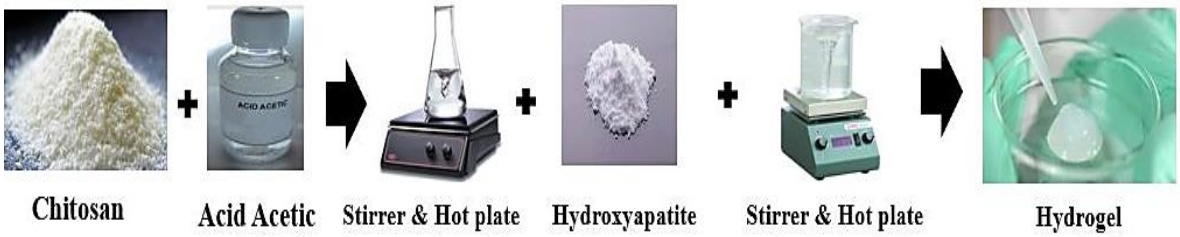

Figure 1: Schematic of preparation of chitosan-hydroxyapatite hydrogel coat.

Then, specific amount of hydroxyapatite (HA) bioceramic with 50-100 nm with 98% purity was poured into the following solution and stirrer for 2 h at 50°C. The porous designed PLA and PCL scaffold were produced using solid work with 2D design, 3D design and FDM method as shown in Figure 2. Thus, a favorable hydrogel (Chitosan-HA) was obtained and a high viscosity hydrogel was developed.

The design file output was STL format and imported into 3D printer software called Simplify 3D. In this software, the 3D printer settings were adjusted during manufacturing process, as well as the output temperature of the nozzle and printer table and its speed. The machine was preheated prior to the printing process and reached the optimum temperature of 200°C for PLA polymer and 60°C for PCL polymer. After reaching to the required temperature, the printing process began. Figure 3 illustrates the process of printing a bone scaffold using FDM 3D printer. After making the chitosan-hydroxyapatite biocomposite coating solution, the samples were coated with soaking the samples in the hydrogel solution for 10 min and then removed from the solution and kept at room temperature. Table 2 shows the mechanical properties results including Poisson's ratio, elastic modulus, density and compressive strength. The samples were fabricated with various amount of HA (S1, S2, S3 and S4) as shown in Table 2.

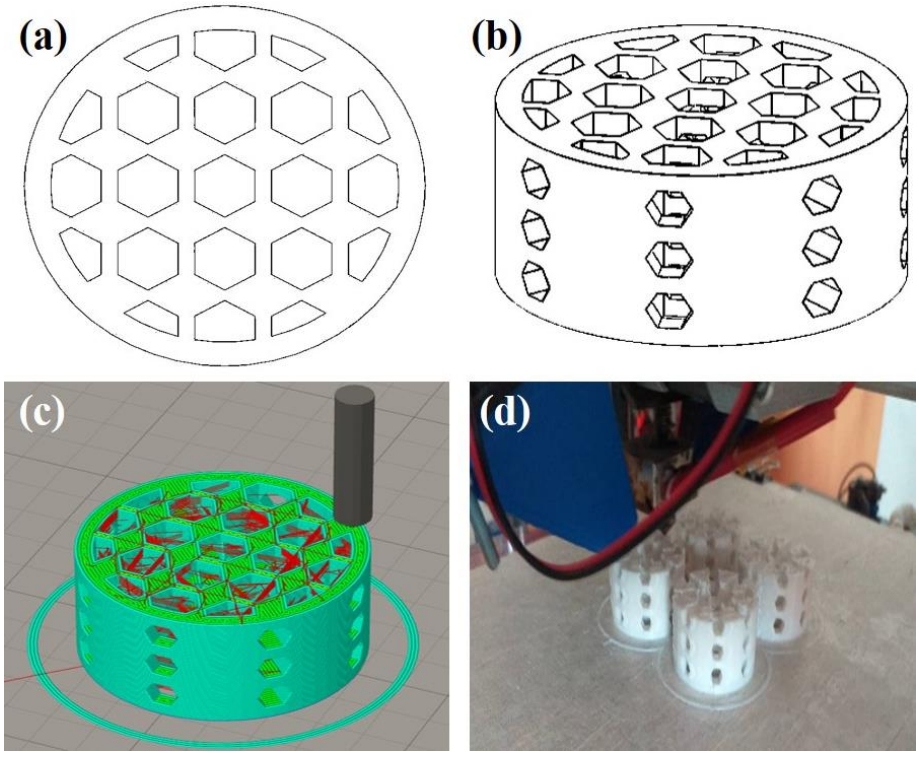

Figure 2: The design of porous (a) 2D top view, (b) lateral view, (c) simplify 3D, and (d) porous architecture of PLA and PCL fabricated using FDM method coated with chitosan-HA.

Table 2: Mechanical properties of porous cylinder scaffolds obtained after mechanical testing and SEM analysis.

Property	S1	S2	S3	S4
Elastic Modulus (MPa)	125	135	142	168
Porosity (%)	65	75	78	80
Compressive strength (MPa)	32	35	38	41
Fracture toughness (MPa.m$^{1/2}$)	0.98	1.2	1.2	1.42

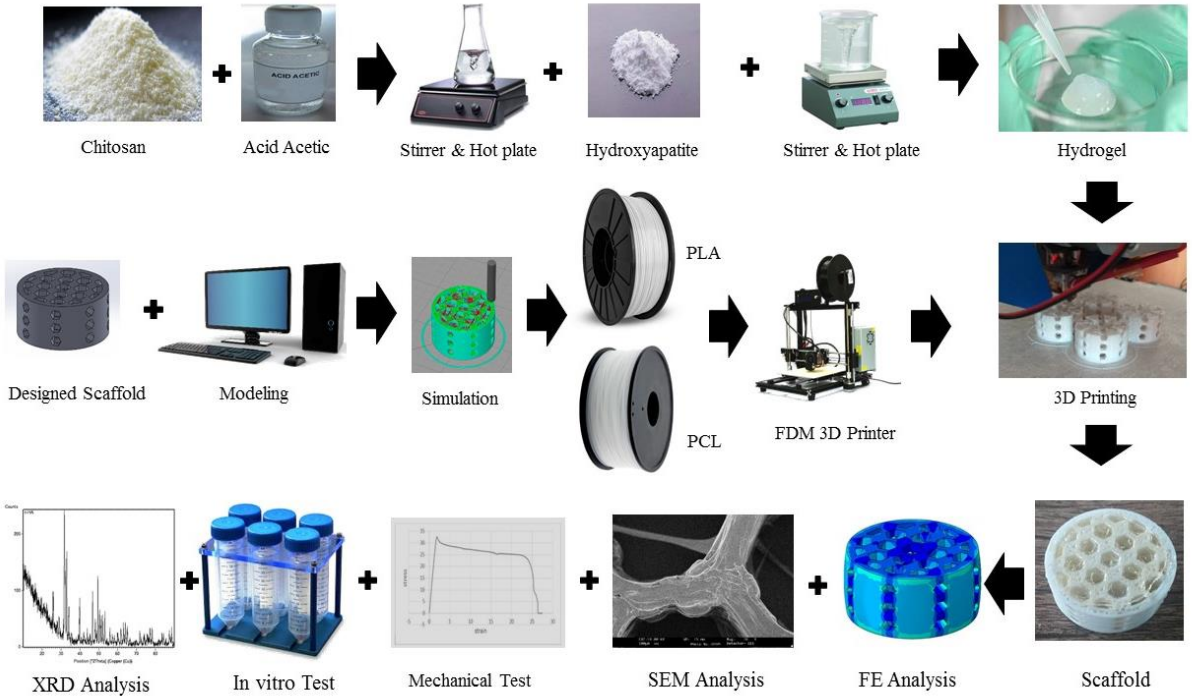

Figure 3: Schematic and overview of preparation of novel porous composite scaffold coated with chitosan polymer.

2.1. Materials characterization of porous scaffold

To determine the phases of the powder and composite scaffold, X-ray diffraction (XRD) were utilizes with Equinox 300 tests in the range of 2θ between 10 and 90° under 40 kV and 30 mA. In order to investigate the morphology and porosity of the scaffold surface, scanning electron microscope (SEM) XI30 Philips was used. Then, the pores of the coated porous composite scaffolds were examined using Image-J software.

2.2. Mechanical testing evaluation

To calculate the mechanical properties of the porous PLA and PCL with chitosan-HA coated under compression test, the SANTAM-STM50 machine was used. For this purpose, each porous cylindrical specimen with a length of 30 mm and a diameter of 10 mm was prepared and loaded at a rate of 0.2 mm/min. The output of the device in the form of force and displacement data was converted to stress and strain curve by having the diameter and initial length of each specimen. Finally, using the elastic region gradient of the stress-strain diagram, the elastic modulus of each sample was obtained. Also, the highest point in the graph showing the greatest stress tolerated by the specimen was considered as the compressive strength of the specimen.

2.3. Porosity evaluation

Liquid displacement method was used to calculate the porosity of porous scaffolds in this project. For this purpose, a graded coted cylinder with a definite volume of distilled water (W_1)

was prepared and the scaffold sample was immersed in the simulated body fluid (SBF). The new volume was named after the immersion cylinder (W_2) and then it was time for the water to penetrate in all the holes and fill them. The filled coated scaffold was then removed and the new volume was called the wet cylinder (W_3). The porosity percentage was calculated according to the fluid displacement method according to the following formula 1.

$$Porosity\ (\%) = \frac{W_1 - W_3}{W_2 - W_3} \times 100 \quad (1)$$

The Image-J software was used to obtain the porosity of the coated sample using at least 20-30 holes in the SEM image too.

2.4. Apatite formation

The swelling properties of the prepared porous scaffolds were studied in an SBF. The simulated body solution was prepared according to the method proposed by Kokubo according to Table 3, in which the concentration of each of the ions in the SBF corresponds to the concentration of ions present in human blood plasma. The solution contains 8 different salts, as shown in Table 3, the type and amount of salts per liter of distilled water. In order to produce one liter of SBF solution, first pour 700 ml of distilled water into one liter and heat up to 36.5°C and then each of the salts given in the previous Table 3 were inserted into the solution.

After adding the salts, the distilled water should be brought to 900 ml and the water temperature controlled to reach 36.5°C. In this case, the pH of the solution should be within the limit of 7.2 ± 1. Then, the Tris based factor is added to reach a pH of 7.3. By controlling the temperature again at the mentioned temperature, the pH was adjusted by adding 1 mM hydrochloric acid (HCl) at 7.45. To investigate the bioactivity property of the scaffolds, the samples were immersed in 10 ml of SBF, prepared as described above, in a water bath at a constant temperature of 37°C (human body temperature) for a period of 28 days. On days 1, 4, 7, 14, 21 and 28, the pH of the solutions containing the samples was measured and recorded with a 162-Meter pH apparatus. The weight of the specimens was also measured by digital scales on the mentioned days. After 28 days, the samples were extracted from the solution and SEM tools was used to evaluate the bioactive properties and morphology of the apatite formed on the scaffolds. The water absorption rate of bone scaffolds is one of the important biological characteristics of these composite materials. For this purpose, scaffolds made with different percentages of polymeric and ceramic phases were cut and weighed in appropriate dimensions and then immersed in distilled water and SBF solution at 37°C.

Table 3: Instructions for the preparation of simulated body fluid solution.

Order	Reagent	Amount	Container	Purity (%)	Formula weight
1	NaCl	8.035 g	Weighing paper	99.5	58.4430
2	$NaHCO_3$	0.355 g	Weighing paper	99.5	84.0068
3	KCl	0.225 g	Weighing bottle	99.5	74.5515
4	$K_2HPO_4.3H_2O$	0.231 g	Weighing bottle	99.0	228.2220
5	$MgCl_2.6H_2O$	0.311 g	Weighing bottle	98.0	203.3034
6	1.0M-HCl	39 ml	Graduated cylinder	-	-
7	$CaCl_2$	0.292 g	Weighing bottle	95.0	110.9848
8	Na_2SO_4	0.072 g	Weighing bottle	99.0	142.0428
9	Tris	6.118 g	Weighing paper	99.0	121.1356
10	1.0M-HCl	0-5 ml	Syringe	-	-

2.5. Abaqus Simulation

To simulate the mechanical properties of the porous scaffold, the extracted data from the mechanical testing were inserted into the Abaqus software to identify scaffolds sensitive points with applying 100 N force, the amount of stress applied to the scaffold and its sensitive points. For simulating the mechanical performance of the porous scaffold using Abaqus software to simulate the static analysis response of the hard tissue. In the design of bone scaffolds, honeycomb modeling was assumed. This porous scaffold with hollow space which exchange bone-forming elements, facilitates the retention of these materials and provides greater strength due to its vertical structure.

3. Results and Discussion

The XRD pattern is used to study the structure of crystalline and non-crystalline materials. The XRD method can be used to determine the size

of the crystals under certain conditions. It is also used to identify crystalline phases and their position of thin multilayers. In this study, materials such as hydroxyapatite and chitosan were used to make composite coatings, as well as PCL and PLA for scaffold preparation using 3D printers. According to the materials used, the validity of the above materials was evaluated and confirmed according to this analysis. Figure 4 (a-d) shows the XRD of hydroxyapatite, chitosan, PCL, and PLA polymer used in the scaffold made by 3D printing technology. First, the specimens were photographed by SEM tools in order to compare the appearance and shape of the holes and their physical properties.

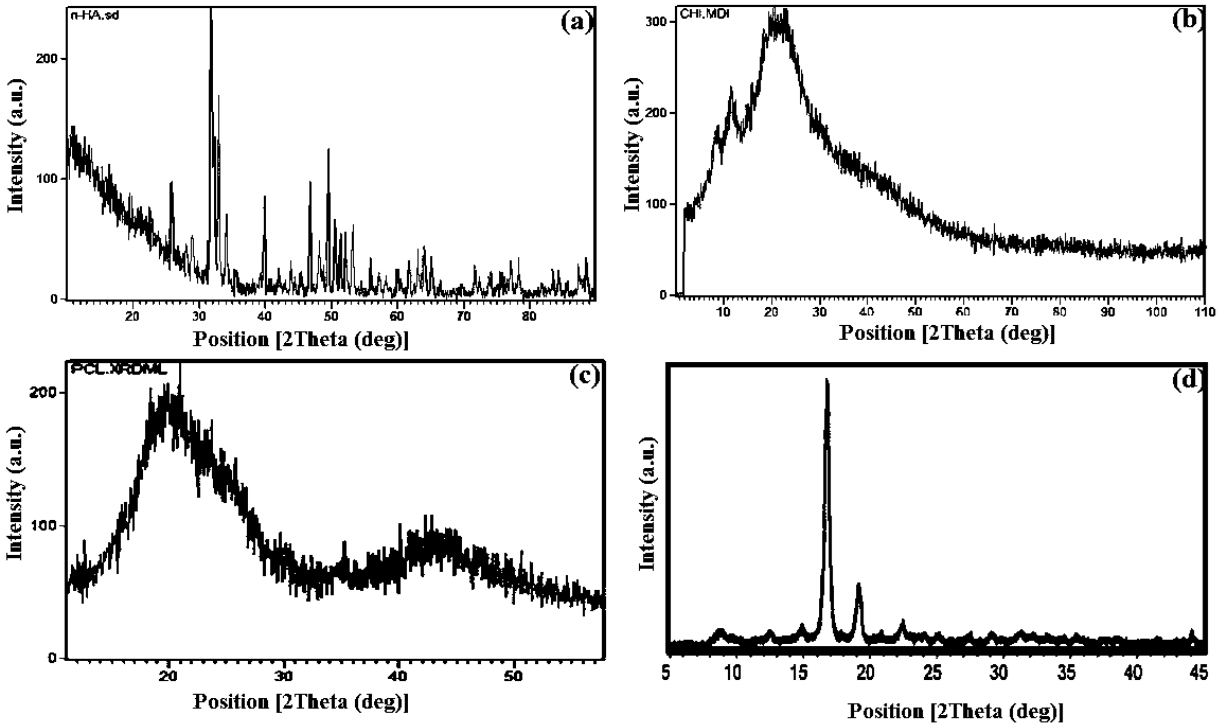

Figure 4: XRD pattern of (a) hydroxyapatite bioceramic, (b) chitosan polymer, (c) polycaprolactone, and (d) Polylactic acid materials.

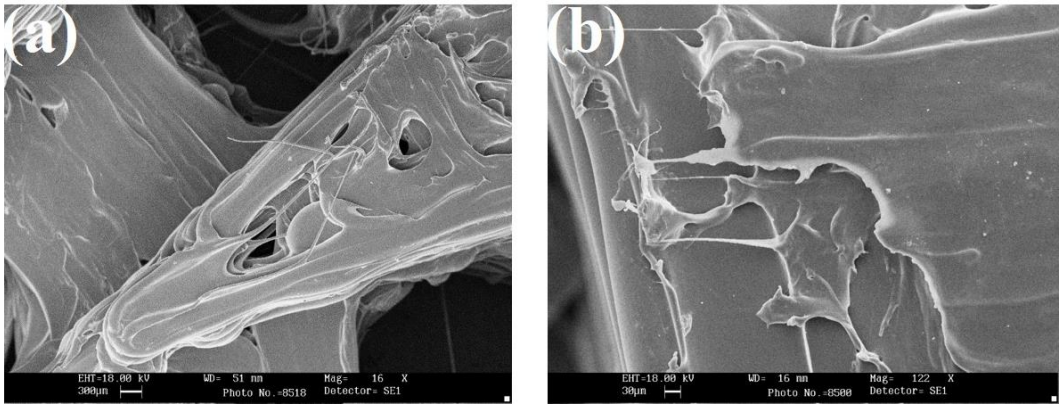

Figure 5: SEM image of porous scaffold coated with chitosan-hydroxyapatite nanoparticles, (a) PLA and (b) PCL.

The SEM images shows the hole are in the range of 50-100 micron. Figure 5 (a-b) shows the SEM image of the fabricated scaffold coated with chitosan-HA nanoparticles made of PLA and PCL. The porosity of the specimens was calculated using Image-J software extracted from the SEM images. Figure 5 (a-b) showed that homogenized HA dispersed in the chitosan

biopolymers. However, the HA mixed with chitosan coated on the PLA better than PCL regarding the low melting temperature of PCL.

Figure 6(a-b) shows the porosity value of the sample with based PLA polymer. It shows that as the base polymer amount can changed it effects on the porosity value. Normally, cortical bones have a compressive strength of 110 to 150 MPa and an elastic modulus of 18 to 22 GPa, whereas the spongy bones have a compressive strength of 2 to 6 MPa and an elastic modulus of 0.1 to 0.3 GPa [25-35].

Mechanical strength is the most important factor in maintaining and stabilizing the scaffold [33-38]. After soaking the samples into the *in vitro* environment, as the bone replaces, this new tissue is affected by different loads in different directions, and if these mechanical loads are not tolerated, the bone scaffold will crack and break down very soon [39-44]. Figure 6 shows that the compressive strength and the fracture toughness of the architecture increased with changing the HA amount in the chitosan polymer from nearly 30 to 40 MPa and 0.9 to 1.5, respectively. This strength is related to several factors such as the materials properties and their strength, the type of reinforcing and mineral particles and their size, the interaction between the organic component and the mineral sediments, as well as the relation of these components [45-52]. The compression test can partially determine the initial strength of the porous scaffolds to mimic with humans' spongy bone [53-57]. The pH of all solutions on the first day was similar to the pH of 7.4. The dissolution of the scaffold in the solutions and their solubility permeated their pH.

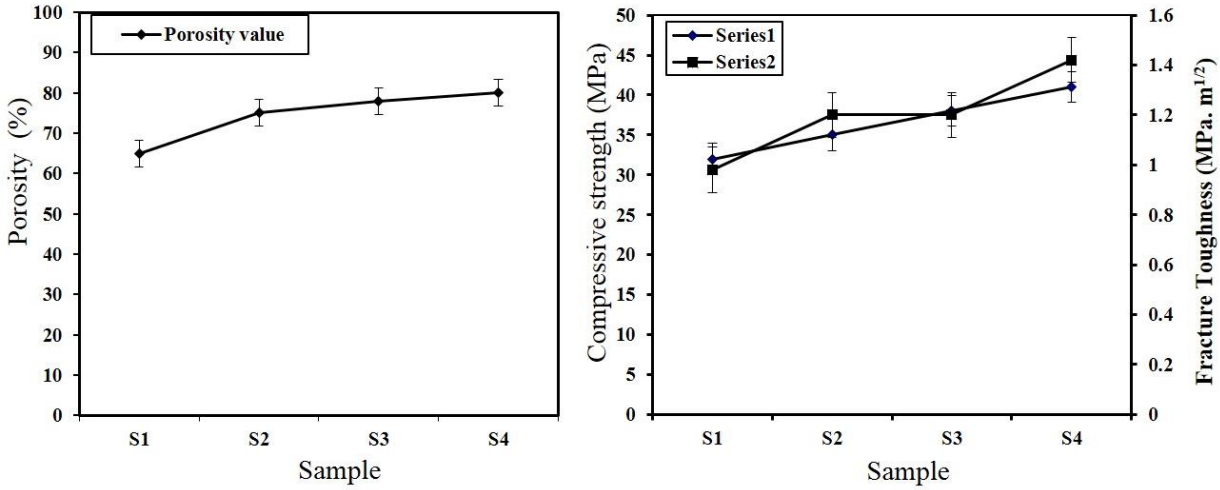

Figure 6: Diagram of (a) Porosity percentages, and (b) compressive strength versus fracture toughness of four specimens coated with chitosan-hydroxyapatite nanoparticles having honeycomb structure.

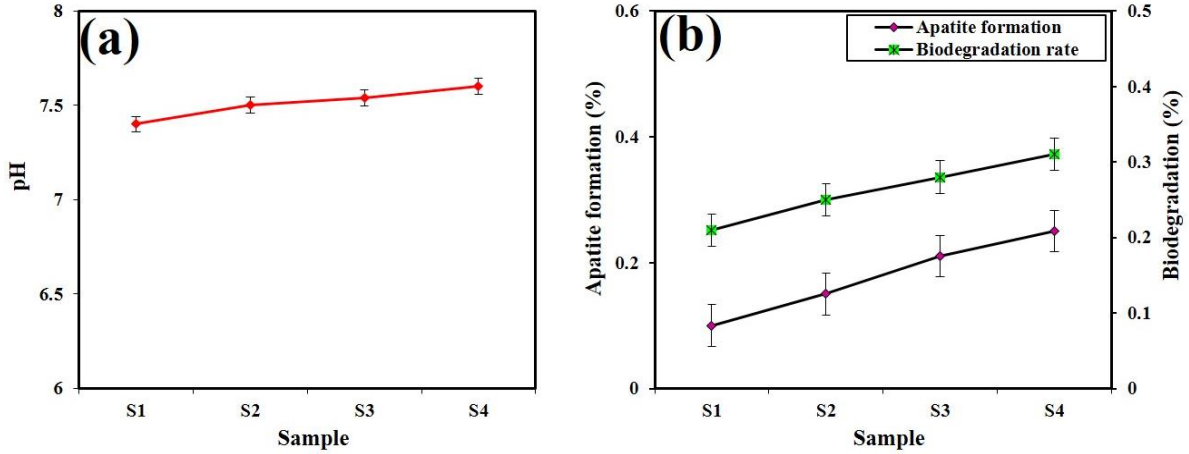

Figure 7: Diagram of (a) pH changes, and (b) apatite formation versus degradation rate in the SBF after 28 days.

Figure 7 (a-b) shows the pH changes in the SBF for 28 days. As it is seen, most of the changes occurred in the first days so that they first decrease and then increases. The obtained results from the biological reaction indicated that after 7 days the pH has reached from 7.4 to 7.7 which can be due to the breakdown of the bonds and release of calcium ions from the scaffold surface after immersion in SBF solution.

The ion displacement in the solution represent the releases of the calcium ions from the scaffold into the solution. The trend of pH changes for all four samples is the same, with a range of less than 0.5, indicating no toxicity in the solution. In Figure 7, the diagram shows the pH changes in the saline solution, which increases over the period of time and continues to increase until 28 day. Based on the pH results, it can be said that 3D scaffolds do not cause toxicity and leads to the pH changes in the blood in such a way as to create an acidic environment. The ability of apatite to form on the scaffold, which facilitates the proper interaction of cells and aligns the antibacterial behavior to the production of bone tissue that can be expected to have good biocompatibility properties at the scaffold site associated with the host tissue [54-59]. The empirical dissolution rate also shows that the sample with zero percent of HA has the highest dissolution rate. Unlike metals and polymers, ceramics can hardly be plastic deformed due to the nature of their bonds and the small amount of sliding systems. These properties make the ceramics nonconductive and have a near-zero creep at room temperature, making the ceramics susceptible to crack propagation and intensity of the microcrack because they elastically break through the crack instead of undergoing plastic deformation. The stress at the crack tip is several times more than the stress in the areas around the material. As a result, the stress concentration causes the material to have weal properties, eventually making it difficult to determine the compression strength of the ceramic material. The scaffolds were designed in the Solid works software by considering the features required for each scaffold and then the model was transferred to the Abaqus software. The analysis performed in Abaqus software was determined as static state and according to the data obtained from compression tests was performed. Regarding the Poisson's coefficient of 0.33, elastic modulus of 3.50 GPa and filament density of 1.25 g/m^3 were set for the material specifications in the Abaqus software. After applying the properties of the material in the software, all constraints below the surface were bound and proper mode was selected. To test the amount of compression value the force applied to the scaffold, a vertical force of 100 N. The simulation was performed with TET meshing structure. The analytical results of the scaffolds showed that by applying force to the scaffold a different distribution of force and stress can be observed at the most sensitive point as shown in Figure 8(a-d). The simulation results showed that the highest stress was of Van Mises Stress (VMS) type at about 13-14 MPa. The barrel shape in all scaffolds was predictable due to their cylindrical shape, with the results supported by the vertical model of force applied as shown in Figure 8 (a-d). According to the shear investigation performed, the inner parts of the scaffold, the stress distribution (cross section) is well illustrated in Figure 8(c). The highest stresses were also applied on the outer edges of the scaffold and in the primitive and bound parts of the scaffold. The analysis confirmed the suitability of the above scaffold. By defining the central point of the scaffold, the stress-strain diagram of the central element shows maximum applied stress to this point is about 5-6 MPa, which is about half the maximum applied stress to the sensitive points of the scaffold as shown in Figure 8(d).

To investigate the effective elastic properties of porous materials, many relationships have been proposed both experimentally and analytically. The analytical methods presented can be broadly divided into two types. The first of these methods is based on theories of composite materials like rule of mixture (ROM). In this group of models, the fragment is considered to be a special case of a composite material with one phase (porosity) having zero stiffness. The second category of these models relates to cell solids. These models are based on solid-surface minimum methods, in which the material is considered to be a single-phase material. The topology, structure and porosity of the scaffold are the factors that contribute to increase and decrease of the compressive strength due to varied loading. One of the shapes and patterns that researchers are interested in because of their

geometry is the high stability and the increase in strength due to the mass-to-volume ratio of the implant. These defects due to the proper distribution of the forces applied to the walls are a factor for the repulsion of the vertical forces, and due to the hexagonal porosity, they can be a suitable factor for the flow of blood and appropriate materials to accelerate bone healing and regeneration. It is natural that as the polymer material changes, the mechanical properties also change, however, with the construction of this scaffold model it can be assured that good strength is achieved with the PLA material.

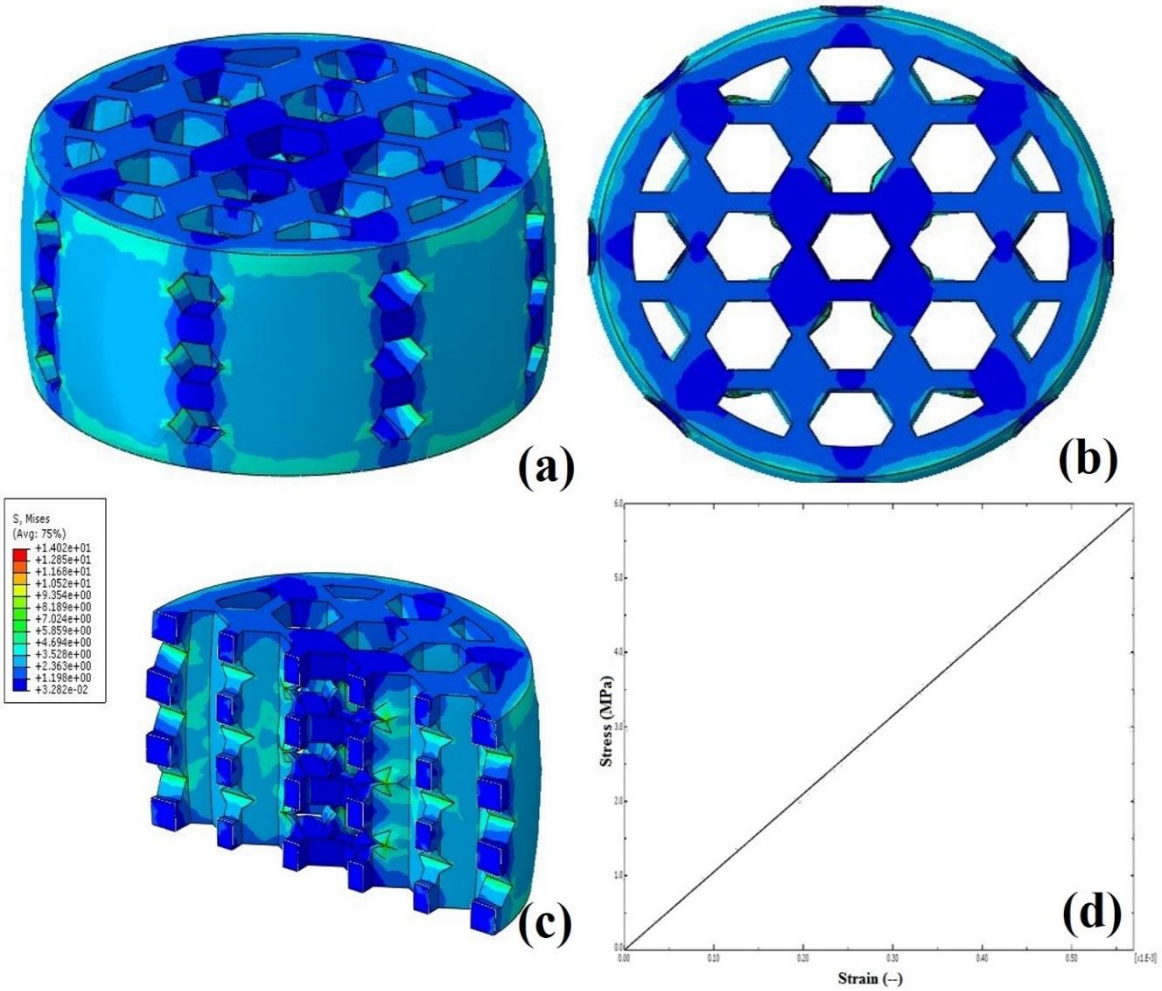

Figure 8: Simulation study of stress distribution applied to the porous bone scaffold prepared using FDM technology (a) lateral view, (b) top view, (c) cross section view, (d) stress-strain diagram in the simulation study of stress distribution after finite element analysis.

4. Conclusion

The obtained results indicated that the compressive strength and elastic modulus increased with changing the HA amount in which the geometry and materials size effects the mechanical properties performance. The SEM images showed that the porosity in the printed scaffolds caused the coating to site well on the scaffold surfaces, and the presence of residual porosity caused the blood, nutrient circulation and apatite growth to form better. The adsorption percentage in saline showed that samples pH does not changed dramatically and have a same trend for all the samples. The obtained XRD results showed that as the HA powder added to the PLA the peak changed to the amorphous structure with a low intensity. As it is seen in the bone structure the path of major stresses occurred in the central of the bulged cylinder. Due to this unique bone feature that

can optimizes scaffold structure, it is recommended to use a computer optimized structure (for better blood and cell nutrition immigration, weight optimization, and feature improvement). The microstructure of the porous scaffold was simulated using the Abaqus software with the extracted data from the experimental work. At the end, it was concluded that the most suitable scaffold was fabricated made of polylactic acid filament and coated with chitosan-hydroxyapatite nanocomposite which can be used in bone tissue engineering applications.

Acknowledgments

The authors received financial support for the research proposal and publication of this article from Young Researchers and Elite Club with 98001 proposal code, Khomeinishahr branch, Islamic Azad University, Isfahan, with the title "Fabrication and analysis of polycaprolactone, polylactic acid- hydroxyapatite bio-nanocomposite scaffolds using 3D FDM printer with hexagonal topology. **Conflict of Interest**

The authors declared no potential conflicts of interest with respect to the research, authorship and publication of this article.

Funding

The authors received financial support for the research proposal and publication of this article from Young Researchers and Elite Club with 98001 proposal code, Khomeinishahr branch, Islamic Azad University, Isfahan, with the title "Fabrication and analysis of polycaprolactone, polylactic acid- hydroxyapatite bio-nanocomposite scaffolds using 3D FDM printer with hexagonal topology.

Reference

1) Esmaeili, S., Shahali, M., Kordjamshidi, A., Torkpoor, Z., Namdari, F., Samandari, S. S., ... & Khandan, A. (2019). An artificial blood vessel fabricated by 3D printing for pharmaceutical application. *Nanomedicine Journal*, *6*(3), 183-194.
2) Khandan, A., & Ozada, N. (2017). Bredigite-Magnetite (Ca7MgSi4O16-Fe3O4) nanoparticles: A study on their magnetic properties. *Journal of Alloys and Compounds*, *726*, 729-736.
3) Khandan, A., Ozada, N., Saber-Samandari, S., & Nejad, M. G. (2018). On the mechanical and biological properties of bredigite-magnetite (Ca7MgSi4O16-Fe3O4) nanocomposite scaffolds. *Ceramics International*, *44*(3), 3141-3148.
4) Monshi, M., Esmaeili, S., Kolooshani, A., Moghadas, B. K., Saber-Samandari, S., & Khandan, A. (2020). A novel three-dimensional printing of electroconductive scaffolds for bone cancer therapy application. *Nanomedicine Journal*, *7*(2), 138-148.
5) Kordjamshidi, A., Saber-Samandari, S., Nejad, M. G., & Khandan, A. (2019). Preparation of novel porous calcium silicate scaffold loaded by celecoxib drug using freeze drying technique: Fabrication, characterization and simulation. *Ceramics International*, *45*(11), 14126-14135.
6) Esmaeili, S., Aghdam, H. A., Motififard, M., Saber-Samandari, S., Montazeran, A. H., Bigonah, M., ... & Khandan, A. (2020). A porous polymeric–hydroxyapatite scaffold used for femur fractures treatment: fabrication, analysis, and simulation. *European Journal of Orthopaedic Surgery & Traumatology*, *30*(1), 123-131.
7) Sahmani, S., Saber-Samandari, S., Khandan, A., & Aghdam, M. M. (2019). Influence of MgO nanoparticles on the mechanical properties of coated hydroxyapatite nanocomposite scaffolds produced via space holder technique: fabrication, characterization and simulation. *Journal of the mechanical behavior of biomedical materials*, *95*, 76-88.
8) Joneidi Yekta, H., Shahali, M., Khorshidi, S., Rezaei, S., Montazeran, A. H., Samandari, S. S., ... & Khandan, A. (2018). Mathematically and experimentally defined porous bone scaffold produced for bone substitute application. *Nanomedicine Journal*, *5*(4), 227-234.
9) Khandan, A., Jazayeri, H., Fahmy, M. D., & Razavi, M. (2017). Hydrogels: Types, structure, properties, and

applications. *Biomat Tiss Eng*, *4*(27), 143-69.

10) Aghdam, H. A., Sanatizadeh, E., Motififard, M., Aghadavoudi, F., Saber-Samandari, S., Esmaeili, S., ... & Khandan, A. (2020). Effect of calcium silicate nanoparticle on surface feature of calcium phosphates hybrid bio-nanocomposite using for bone substitute application. *Powder Technology*, *361*, 917-929.
11) Farazin, A., Aghdam, H. A., Motififard, M., Aghadavoudi, F., Kordjamshidi, A., Saber-Samandari, S., & Khandan, A. (2019). A polycaprolactone bio-nanocomposite bone substitute fabricated for femoral fracture approaches: Molecular dynamic and micro-mechanical Investigation. *J Nanoanaly*.
12) Montazeran, A. H., Saber Samandari, S., & Khandan, A. (2018). Artificial intelligence investigation of three silicates bioceramics-magnetite bio-nanocomposite: Hyperthermia and biomedical applications. *Nanomedicine Journal*, *5*(3), 163-171.
13) Esmaeili, S., Khandan, A., & Saber-Samandari, S. (2018). Mechanical performance of three-dimensional bio-nanocomposite scaffolds designed with digital light processing for biomedical applications. *Iranian Journal of Medical Physics*, *15*, 328-328.
14) Hashemi, S. A., Esmaeili, S., Ghadirinejad, M., Saber-Samandari, S., Sheikhbahaei, E., Kordjamshidi, A., & Khandan, A. (2020). Micro-Finite Element Model to Investigate the Mechanical Stimuli in Scaffolds Fabricated via Space Holder Technique for Cancellous Bone. *ADMT Journal*, *13*(1), 51-58.
15) Farazin, A., Aghadavoudi, F., Motififard, M., Saber-Samandari, S., & Khandan, A. (2020). Nanostructure, molecular dynamics simulation and mechanical performance of PCL membranes reinforced with antibacterial nanoparticles. *Journal of Applied and Computational Mechanics*.
16) Sahmani, S., Khandan, A., Saber-Samandari, S., & Aghdam, M. M. (2020). Effect of magnetite nanoparticles on the biological and mechanical properties of hydroxyapatite porous scaffolds coated with ibuprofen drug. *Materials Science and Engineering: C*, 110835.
17) Maghsoudlou, M. A., Nassireslami, E., Saber-Samandari, S., & Khandan, A. (2020). Bone Regeneration Using Bio-Nanocomposite Tissue Reinforced with Bioactive Nanoparticles for Femoral Defect Applications in Medicine. *Avicenna Journal of Medical Biotechnology*, *12*(2).
18) Ghayour, H., Abdellahi, M., Nejad, M. G., Khandan, A., & Saber-Samandari, S. (2018). Study of the effect of the Zn 2+ content on the anisotropy and specific absorption rate of the cobalt ferrite: the application of Co 1− x Zn x Fe 2 O 4 ferrite for magnetic hyperthermia. *Journal of the Australian Ceramic Society*, *54*(2), 223-230.
19) Seitz, H., Rieder, W., Irsen, S., Leukers, B., & Tille, C. (2005). Three-dimensional printing of porous ceramic scaffolds for bone tissue engineering. Journal of Biomedical Materials Research Part B: Applied Biomaterials: An Official Journal of The Society for Biomaterials, The Japanese Society for Biomaterials, and The Australian Society for Biomaterials and the Korean Society for Biomaterials, 74(2), 782-788.
20) Kamyab Moghadas, B., & Azadi, M. (2019). Fabrication of Nanocomposite Foam by Supercritical CO2 Technique for Application in Tissue Engineering. *Journal of Tissues and Materials*, *2*(1), 23-32.
21) Rad, A. S., Samipour, V., Movaghgharnezhad, S., Mirabi, A., Shahavi, M. H., & Moghadas, B. K. (2019). X12N12 (X= Al, B) clusters for protection of vitamin C; molecular modeling investigation. *Surfaces and Interfaces*, *15*, 30-37.
22) Moghadas, B. K., Akbarzadeh, A., Azadi, M., Aghili, A., Rad, A. S., &

Hallajian, S. (2020). The morphological properties and biocompatibility studies of synthesized nanocomposite foam from modified polyethersulfone/graphene oxide using supercritical CO2. *Journal of Macromolecular Science, Part A*, *57*(6), 451-460.

23) Shahriari, S., Houshmand, B., Razavian, H., Khazaei, S., & Abbas, F. M. (2012). Effect of the combination of enamel matrix derivatives and deproteinized bovine bone materials on bone formation in rabbits' calvarial defects. *Dental research journal*, *9*(4), 422.
24) Ghasemi, E., Abedian, A., Iranmanesh, P., & Khazaei, S. (2015). Effect of type of luting agents on stress distribution in the bone surrounding implants supporting a three-unit fixed dental prosthesis: 3D finite element analysis. *Dental research journal*, *12*(1), 57.
25) Khazaei, S., Firouzei, M. S., Afghari, P., & Khazaei, M. (2014). Resveratrol may improve osseointegration of dental implants in type 2 diabetes mellitus patients. *J Res Med Sci*, *19*(1), 81.
26) Hasheminia, D., Razavi, S. M., Nazari, H., Khazaei, S., & Soleimanzadeh, P. (2018). Systemic supplement with resveratrol increased bone formation in ratsâ alveolar socket Aumento de la formaciÃ³n Ã³sea en el hueso alveolar de rata con suplemento sistÃ© mico con resveratrol. *International Journal of Morphology*, *36*(2), 391-394.
27) Moeini, M., Barbaz Isfahani, R., Saber-Samandari, S., & Aghdam, M. M. (2020). Molecular dynamics simulations of the effect of temperature and strain rate on mechanical properties of graphene–epoxy nanocomposites. *Molecular Simulation*, *46*(6), 476-486.
28) Maghsoudlou, M. A., Isfahani, R. B., Saber-Samandari, S., & Sadighi, M. (2019). Effect of interphase, curvature and agglomeration of SWCNTs on mechanical properties of polymer-based nanocomposites: Experimental and numerical investigations. *Composites Part B: Engineering*, *175*, 107119.
29) Barbaz-I, R. (2014). *Experimental determining of the elastic modulus and strength of composites reinforced with two nanoparticles* (Doctoral dissertation, MSc Thesis, School of Mechanical Engineering Iran University of Science and Technology, Tehran, Iran).
30) Monfared, R. M., Ayatollahi, M. R., & Isfahani, R. B. (2018). Synergistic effects of hybrid MWCNT/nanosilica on the tensile and tribological properties of woven carbon fabric epoxy composites. *Theoretical and Applied Fracture Mechanics*, *96*, 272-284.
31) Ayatollahi, M. R., Barbaz Isfahani, R., & Moghimi Monfared, R. (2017). Effects of multi-walled carbon nanotube and nanosilica on tensile properties of woven carbon fabric-reinforced epoxy composites fabricated using VARIM. *Journal of Composite Materials*, *51*(30), 4177-4188.
32) Ayatollahi, M. R., Moghimi Monfared, R., & Barbaz Isfahani, R. (2019). Experimental investigation on tribological properties of carbon fabric composites: effects of carbon nanotubes and nano-silica. *Proceedings of the Institution of Mechanical Engineers, Part L: Journal of Materials: Design and Applications*, *233*(5), 874-884.
33) Razmjooee, K., Saber-Samandari, S., Keshvari, H., & Ahmadi, S. (2019). Improving anti thrombogenicity of nanofibrous polycaprolactone through surface modification. *Journal of biomaterials applications*, *34*(3), 408-418.
34) Zamani, D., Razmjooee, K., Moztarzadeh, F., & Bizari, D. Synthesis and Characterization of Alginate Scaffolds Containing Bioactive Glass for Bone Tissue Engineering Applications. In *2017 24th National and 2nd International Iranian Conference on Biomedical Engineering (ICBME)* (pp. 330-333). IEEE.
35) Saber-Samandari, S., Yekta, H., Ahmadi, S., & Alamara, K. (2018). The

role of titanium dioxide on the morphology, microstructure, and bioactivity of grafted cellulose/hydroxyapatite nanocomposites for a potential application in bone repair. *International journal of biological macromolecules*, *106*, 481-488.

36) Saber-Samandari, S., Yekta, H., & Saber-Samandari, S. (2015). Effect of iron substitution in hydroxyapatite matrix on swelling properties of composite bead. *JOM*, *9*(1), 19-25.
37) Moradi-Dastjerdi, R., Malek-Mohammadi, H., & Momeni-Khabisi, H. (2017). Free vibration analysis of nanocomposite sandwich plates reinforced with CNT aggregates. *ZAMM-Journal of Applied Mathematics and Mechanics/Zeitschrift für Angewandte Mathematik und Mechanik*, *97*(11), 1418-1435.
38) Salami, M. A., Kaveian, F., Rafienia, M., Saber-Samandari, S., Khandan, A., & Naeimi, M. (2017). Electrospun polycaprolactone/lignin-based nanocomposite as a novel tissue scaffold for biomedical applications. Journal of medical signals and sensors, 7(4), 228.
39) Moradi-Dastjerdi, R., & Aghadavoudi, F. (2018). Static analysis of functionally graded nanocomposite sandwich plates reinforced by defected CNT. *Composite Structures*, *200*, 839-848.
40) Bagheri, S., Hashemian, M., Khosravi, M., & Khandan, A. (2020). An experimental investigation of novel hybrid epoxy/glass fibers nanocomposite reinforced with nanoclay with enhanced properties for low velocity impact test. *Journal of Nanostructures*, *10*(1), 92-106.
41) Azizi, M., Azimzadeh, M., Afzali, M., Alafzadeh, M., & Mirhosseini, S. H. (2018). Characterization and optimization of using calendula offlcinalis extract in fabrication of polycaprolactone-gelatin electrospun nanofibers for wound dressing applications. *Journal of Advanced Materials and Processing*, *6*(2), 34-46.
42) Bafandeh, M. R., Gharahkhani, R., & Fathi, M. H. (2016). Fabrication, Characterization and Osteoblast Response of Cobalt-Based Alloy/Nano Bioactive Glass Composites. *J. Adv. Mater. Process*, *4*, 3-13.
43) Torkan, E., Pirmoradian, M., & Hashemian, M. (2019). Instability inspection of parametric vibrating rectangular Mindlin plates lying on Winkler foundations under periodic loading of moving masses. *Acta Mechanica Sinica*, *35*(1), 242-263.
44) Sourani, P., Hashemian, M., Pirmoradian, M., & Toghraie, D. (2020). A comparison of the Bolotin and incremental harmonic balance methods in the dynamic stability analysis of an Euler–Bernoulli nanobeam based on the nonlocal strain gradient theory and surface effects. *Mechanics of Materials*, 103403.
45) Sahmani, S., Khandan, A., Esmaeili, S., Saber-Samandari, S., Nejad, M. G., & Aghdam, M. M. (2020). Calcium phosphate-PLA scaffolds fabricated by fused deposition modeling technique for bone tissue applications: Fabrication, characterization and simulation. *Ceramics International*, *46*(2), 2447-2456.
46) Ghasemi, M., Nejad, M. G., & Bagzibagli, K. (2017). Knowledge Management Orientation: An Innovative Perspective to Hospital Management. *Iranian journal of public health*, *46*(12), 1639.
47) Ghadirinejad, M., Atasoylu, E., Izbirak, G., & Ghasemi, M. (2016). A Stochastic Model for the Ethanol Pharmacokinetics. *Iranian journal of public health*, *45*(9), 1170.
48) Abdellahi, M., Najafinezhad, A., Ghayour, H., Saber-Samandari, S., & Khandan, A. (2017). Preparing diopside nanoparticle scaffolds via space holder method: Simulation of the compressive strength and porosity. Journal of the mechanical behavior of biomedical materials, 72, 171-181.

49) Sahmani, S., Shahali, M., Nejad, M. G., Khandan, A., Aghdam, M. M., & Saber-Samandari, S. (2019). Effect of copper oxide nanoparticles on electrical conductivity and cell viability of calcium phosphate scaffolds with improved mechanical strength for bone tissue engineering. *The European Physical Journal Plus*, *134*(1), 7.
50) Bahadori, M., Yaghoubi, M., Haghgoshyie, E., Ghasemi, M., & Hasanpoor, E. (2019). Patients' and physicians' perspectives and experiences on the quality of medical consultations: a qualitative evidence. *International journal of evidence-based healthcare*.
51) Khandan, A., Karamian, E., & Bonakdarchian, M. (2014). Mechanochemical synthesis evaluation of nanocrystalline bone-derived bioceramic powder using for bone tissue engineering. *Dental Hypotheses*, *5*(4), 155.
52) Staninec, M., & Tsuji, G. H.. Restoration of non-carious cervical lesions with ceramic inlays: A possible model for clinical testing of adhesive cements. Dent. Hypotheses 2012, 3(4), 155.
53) Zou, D., Zhu, S., Zhou, J., He, J., Wang, Y., Xie, Z., ... & Huang, Y.. Hypoxia-Inducible Factor-1α: A Potential Factor for the Enhancement of Osseointegration between Dental Implants and Tissue-Engineered Bone. Dent. Hypotheses, 2011, 2(3).
54) Zhuang, Q. W., Zhang, Z. Y., Liu, G. L., Fu, S. T., & He, Y. (2013). Transforming growth factor-β1/Smad/connective tissue growth factor axis: The main pathway in radiation-induced fibrosis of osteoradionecrosis?. Dent. Hypotheses, (2013) 4(4), 122.
55) Meraji, N., Bolhari, B., Sefideh, M. R., & Niavarzi, S. Prevention of Tooth Discoloration Due to Calcium-Silicate Cements: A Review. Dent. Hypotheses, 2019, 10(1), 4.
56) Saber-Samandari, S., Saber-Samandari, S., Ghonjizade-Samani, F., Aghazadeh, J., & Sadeghi, A. (2016). Bioactivity evaluation of novel nanocomposite scaffolds for bone tissue engineering: The impact of hydroxyapatite. Ceramics International, 42(9), 11055-11062.
57) Afshary, K., Chamanara, M., Talari, B., Rezaei, P., & Nassireslami, E. (2020). Therapeutic Effects of Minocycline Pretreatment in the Locomotor and Sensory Complications of Spinal Cord Injury in an Animal Model. *Journal of Molecular Neuroscience*, 1-9.
58) Zarei, M. H., Pourahmad, J., & Nassireslami, E. (2019). Toxicity of arsenic on isolated human lymphocytes: The key role of cytokines and intracellular calcium enhancement in arsenic-induced cell death. *Main Group Metal Chemistry*, *42*(1), 125-134.
59) Nassireslami, E., & Ajdarzade, M. (2018). Gold coated superparamagnetic iron oxide nanoparticles as effective nanoparticles to eradicate breast cancer cells via photothermal therapy. *Advanced pharmaceutical bulletin*, *8*(2), 201.